The malachite-rosasite group: crystal structures of glaukosphaerite and pokrovskite

NATALE PERCHIAZZI*, STEFANO MERLINO

Dipartimento di Scienze della Terra, Università di Pisa, Via S. Maria 53, 56126 Pisa, Italy
*Corresponding author, e-mail: natale@dst.unipi.it

Abstract: The crystal structures of glaukosphaerite $(Cu,Ni)_2(CO_3)(OH)_2$ and pokrovskite $Mg_2(CO_3)(OH)_2$, two carbonates belonging to the malachite-rosasite group, have been determined from powder diffraction data, and refined up to $wRp = 3.94\%$ and 1.63% respectively. Both minerals are isostructural with rosasite $(Cu,Zn)_2(CO_3)(OH)_2$, with $P2_1/a$ space group and cell parameters $a = 12.0613(4)$ Å, $b = 9.3653(4)$, $c = 3.1361(1)$, $\beta = 98.085(5)°$ for glaukosphaerite and $a = 12.2396(4)$, $b = 9.3506(4)$, $c = 3.1578(1)$, $\beta = 96.445(5)°$ for pokrovskite.

Their structures are built up by ribbons of edge-sharing octahedra running along the c-axis; the ribbons are linked together through corner-sharing giving rise to corrugated layers parallel to (100) that are interconnected through carbonate groups. The same layers and carbonate groups, arranged in a different orientation with respect to the symmetry operators, build up the structure of malachite: the relationships between the rosasite-like and the malachite-like structural models are discussed. The octahedral distortion of the two independent Me sites in the malachite-rosasite known structures is evaluated and attributed to the Jahn-Teller effect of Cu^{2+}. According to the available chemical data for the examined material, a partial occupancy in Mg sites of pokrovskite is maintained, with a coupled partial substitution of hydroxyls by water molecules. On the basis of the structural results, the difficulties and ambiguities in the powder pattern indexing by preceeding authors are discussed and explained, and reliable guesses for the arrangements of kolwezite and nullaginite are drawn.

Key-words: glaukosphaerite, pokrovskite, powder data, structural solution, malachite-rosasite group.

Introduction

Several phases, with general crystal chemical formula $Me_2^{2+}(CO_3)(OH)_2$, can be grouped in the malachite-rosasite group of minerals: common minerals, such as malachite $(Me^{2+}= Cu)$ and rosasite $(Me^{2+}= Cu, Zn)$, are present, together with rare species such as mcguinnessite (Mg,Cu), glaukosphaerite (Cu,Ni), kolwezite (Cu,Co), nullaginite (Ni), pokrovskite (Mg), zincrosasite (Zn,Cu) and the phase $Fe_2(CO_3)(OH)_2$, recently found in the Dronino meteorite (Burke & Ferraris, 2005).

The similarities of the powder patterns of the various phases, suggest close structural relationships between these phases. Space group symmetry and cell parameters determined through single crystal studies have been obtained for malachite and rosasite only. The crystallographic data of the other phases, which are constantly found as microcrystalline fibrous aggregates, were based on powder pattern indexing and present some degree of uncertainty.

It has been shown (Perchiazzi, 2006) that both malachite and rosasite structures are built up by the same "modules", namely "octahedral" walls of edge-sharing Me^{2+} polyhedra, linked together through corner sharing to form infinite layers, and "triangular" CO_3 groups, which assure their inter-

layer connection. Two distinct structural models are so realized in this mineral group, henceforth denoted as malachite-like and rosasite-like structures.

Glaukosphaerite was defined as new species by Price & Just (1974) who indicated for the specimen from the type locality (Kambalda, Zaire) the ideal formula $(Cu,Ni)_2(CO_3)(OH)_2$ and the unit cell parameters $a = 9.34$, $b = 11.93$, $c = 3.07$ Å, $\beta = 90–91°$ (monoclinic with indeterminate space group). Several lines in the powder pattern cannot be indexed with these parameters; to overcome this problem Jambor (1976) pointed to a slightly higher β value (92.54°) and an unreasonably high c value (3.413 Å), whereas Deliens & Piret (1980) pointed to a triclinic cell (specimen from Kasompi, Zaire). Nickel & Berry (1981) re-examined samples of glaukosphaerite from Kasompi and maintained that two phases were present, one orthorhombic (A centred cell $a = 9.354$, $b = 23.954$, $c = 3.128$ Å) and the other monoclinic ($a = 9.35$, $b = 11.97$, $c = 3.13$ Å, $\beta = 96°$). According to Nickel & Berry (1981) the monoclinic phase may correspond to a nickeloan variety of malachite.

Pokroskvite was defined as new mineral by Ivanov *et al.* (1984) from the Zlatorgoskaya intrusion in central Kazakhstan. The unit cell parameters were calculated on the basis of powder diffraction data, assuming isostructurality with

malachite, as $a = 9.43$, $b = 12.27$, $c = 3.395$ Å, $\beta = 96.6°$. Pokrovskite has been found at several North American localities, although its actual nature had not been realized (White, 1987). A description of pokrovskite from four North American localities, all occurrences being within ultramafic bodies of dunite or serpentinite, has been presented by Fitzpatrick (1986). Günter & Oswald (1977) presented evidences for topotactic formation of $Mg_2(CO_3)(OH)_2$ as intermediate product in the thermal decomposition of artinite $Mg_2(CO_3)(OH)_2 \cdot 3H_2O$ and determined the following unit cell dimensions: $a = 9.34$, $b = 3.15$, $c = 12.18$ Å, $\beta = 90°$.

This study aims to reliably define the crystallographic data of glaukosphaerite and pokrovskite and to determine which structural model they actually display.

Experimental

Glaukosphaerite from Carr Boyd mine, Australia (Pryce & Just, 1974), kindly provided by R. Pogson, the Australian Museum, Sydney, together with a pokrovskite specimen from Sonoma County, California (Fitzpatrick, 1986), were tested in the present investigation. The material for study was carefully selected with the aid of both a polarizing and a binocular microscope, to avoid the presence of impurities, and gently hand ground under acetone in an agate mortar. The resulting powder was loaded into a borosilicate Lindemann capillary 0.4 mm in diameter.

Scans were recorded for both glaukosphaerite and pokrovskite on a D8 Advance Bruker diffractometer, equipped with a primary Ge(111) monochromator ($\lambda = 1.54096$ Å) and a PSD linear detector. Datasets were collected working in rotating capillary geometry, so to minimize preferred orientation effects, in the range 11–100° 2θ, with step size 0.0156° and counting time 36 seconds.

Rietveld refinement of glaukosphaerite and pokrovskite

For both glaukosphaerite and pokrovskite trials were made to refine in a malachite-like setting, using the malachite atomic coordinates (Zigan *et al.*, 1977) as a starting model, and through the structure solution option in TOPAS-Academic (Coelho, 2004) and EXPO2004 (Altomare *et al.*, 2004), but no reasonable result was obtained. A rosasite-like starting model was then assumed for both phases, and the cell setting given for rosasite by Roberts *et al.* (1986) was transformed through the [102/0 $\bar{1}$ 0/00 $\bar{1}$] matrix to obtain the following unit cell parameters: $a = 12.2413$, $b = 9.3705$, $c = 3.1623$ Å, $\beta = 98.73°$, with space group $P\,2_1/a$ [this orientation is preferable due to the smaller β angle]. Rietveld refinements for both glaukosphaerite and pokrovskite were performed with the TOPAS-Academic program (Coelho, 2004), using the fundamental parameter method as implemented in TOPAS (Cheary & Coelho, 1992, 1998). For both phases, a Pawley refinement (Pawley, 1981) was initially performed to get starting values for background, cell parameters, asymmetry and peak shapes. The background was

modeled with a $\frac{1}{x}$ function, effective to describe background intensity at low angles due to air scattering, and a 8-terms Chebyschev function. Absorption corrections for intensity and 2θ peak position were applied, according to the formulation for a cylindrical sample given by Sabine *et al.* (1998). A low degree of preferred orientation, due to the acicular [001] habit of glaukosphaerite, was detected and corrected, following the formulation of March revised by Dollase (1986).

In the early stages of the two refinements, constraints on the Me-O bonds were introduced; these constraints were finally removed in the last refinement cycles. The carbonate group was refined as a rigid body, assuming a C-O distance of 1.3 Å (Zemann, 1981). Isotropic displacement parameters were refined for all the atoms, with like atoms constrained to the same value.

In glaukosphaerite, a full occupancy by copper for Me1 site, and a mixed occupancy $Cu_{0.5}Ni_{0.5}$ for the Me2 site were assumed (Pryce & Just, 1974). A full Mg occupancy was firstly assumed for octahedral sites in pokrovskite. Starting from the rosasite model, the structure of glaukosphaerite was refined up to $Rp = 2.85\%$, $wRp = 3.94\%$. As regards pokrovskite a relatively high isotropic displacement parameter was obtained for the Mg cations, $B_{eq} = 2.0$ Å^2 with respect to $B_{eq} = 0.55$ Å^2 for the octahedral cations in glaukosphaerite. Taking into account also the chemical data presented by Ivanov *et al.* (1985) and Fitzpatrick (1986) (see discussion) the final refinement cycles were carried on assuming a Mg occupancy of 0.88, obtaining for Mg atoms a $B_{eq} = 1.0$ Å^2; the final reliability indices for pokrovskite refinement were: $Rp = 1.14\%$, $wRp = 1.63\%$.

Experimental data are available from the authors upon request.

Structure description

Refined cell parameters for glaukosphaerite and pokrovskite are reported in Table 1, together with crystallographic data for the other phases of this group. Final atomic coordinates and isotropic displacement parameters for the two structures are reported in Table 2, and the geometry of the coordination polyhedra of the two independent Me sites is given in Table 3.

As already noticed by Perchiazzi (2006) in his study of the structures of rosasite and mcguinessite, a clear distinction is possible between the larger, more distorted Me1 octahedron, and the smaller, more regular Me2 octahedron. This is especially evident in glaukosphaerite, whose Me1 polyhedron, fully occupied by Cu, displays the common (4+2) coordination, due to the Jahn-Teller effect. Two oxygens and two hydroxyls are arranged in nearly square coordination, with $<$Cu-O$>$ 2.011 Å; two further oxygens complete the distorted octahedra. In accordance with the regular octahedral coordination expected for Ni^{2+}, Me2 polyhedron, with $<$Me-O$>$ 2.078 Å, is more regular and its distortion is due to the partial substitution of Ni^{2+} by Cu^{2+} in this site. Me1 and Me2 octahedra in pokrovskite are quite regular, with $<$Me-O$>$ distances 2.146 and 2.117 Å respectively. Comparing the volume of Me1 and Me2 polyhedra (Table 4)

Table 1. Crystallography of the phases of the malachite-rosasite group (Å,°). Besides malachite, the phases with an established rosasite-like structure are shown together, and lastly minerals with still unknown structure are reported.

Phase	sp. gr.	a	b	c	β	Ref.
Malachite	$P\,2_1/a\,1\,1$	11.974	9.502	3.240	98.75	(1)
Mcguinnessite	$P\,1\,2_1/a\,1$	12.1531(3)	9.3923(3)	3.1622(1)	97.784(4)	(2)
Rosasite	$P\,1\,2_1/a\,1$	12.2413(2)	9.3705(2)	3.1612(2)	98.730(3)	(2)
Glaukosphaerite	$P\,1\,2_1/a\,1$	12.0613(4)	9.3653(4)	3.1361(1)	98.085(5)	(3)
Pokrovskite	$P\,1\,2_1/a\,1$	12.2396(4)	9.3506(4)	3.1578(1)	96.445(5)	(3)
Kolwezite	triclinic	9.500	12.150	3.189		(4)
		α= 93.32	β= 90.74	γ= 91.47		
Nullaginite	$P\,2_1/m\,1\,1$	12.001	9.236	3.091	90.48	(5)
$Fe_2(CO_3)(OH)_2$	orthorhombic	9.390	24.53	3.212		(6)

(1): Zigan *et al.*, 1977; (2) Perchiazzi, 2006; (3) This study; (4) Deliens & Piret, 1980; (5) Nickel & Berry, 1981; (6) Erdös & Altorfer (1976).

Table 2. Final fractional atomic coordinates and isotropic displacement parameters for glaukosphaerite and pokrovskite.

	Me1	Me2	C	O1	O2	O3	OH4	OH5
				Pokrovskite				
x	0.2122(4)	0.3989(4)	0.1503	0.1499	0.2400	0.0612	0.3656(5)	0.4294(4)
y	0.0045(5)	0.7710(5)	-0.2637	-0.1279	-0.3377	-0.3249	0.9162(6)	0.6266(6)
z	0.983(2)	0.574(1)	0.5365	0.4448	0.5307	0.6339	0.062(2)	0.103(2)
B_{eq}	1.0(1)	1.0(1)	5.9(4)	3.0(1)	3.0(1)	3.0(1)	3.0(1)	3.0(1)
				Glaukosphaerite				
x	0.2129(2)	0.3901(2)	0.1360	0.1284	0.2324	0.0473	0.3504(7)	0.4216(6)
y	0.9979(4)	0.7675(3)	-0.2716	-0.1357	-0.3354	-0.3437	0.9024(8)	0.6241(9)
z	0.991(1)	0.6112(9)	0.5943	0.5116	0.6193	0.6521	0.038 (4)	0.113(4)
B_{eq}	0.55(5)	0.55(5)	1.7(5)	0.8(1)	0.8(1)	0.8(1)	0.8(1)	0.8(1)

Table 3: Bond distances (Å) in Me1 and Me2 coordination polyhedra of glaukosphaerite and pokrovskite. For glaukosphaerite, angles (°) of the quadratic coordination of copper are also reported.

Pokrovskite		Glaukosphaerite		?	
Me1 - OH4	2.041(6)	OH4	1.871(8)	OH4-Cu1-O1	96.3(5)
OH5	2.068(5)	OH5	1.997(8)	OH5-Cu1-O2	80.3(5)
O1	2.118(9)	O2	2.03(1)	OH5-Cu1-O1	87.7(6)
O2	2.161(7)	O1	2.11(1)	OH4-Cu1-O2	96.2(5)
O1	2.172(7)	mean	2.002		
O2	2.317(9)	O1	2.40(2)		
mean	2.146	O2	2.62(1)		
Me2 - O3	2.041(7)	OH4	1.95(1)		
OH5	2.086(8)	O3	2.01(1)		
OH4	2.098(6)	OH5	2.06(1)		
OH4	2.117(6)	O2	2.13(1)		
OH5	2.164(7)	OH5	2.13(1)		
O2	2.187(7)	OH4	2.19(1)		
mean	2.115	mean	2.078		

derived from available structural refinements, one can notice that, in all the investigated structures, the Me1 octahedra are constantly larger than Me2 octahedra, and that, both for Me1 and Me2, the polyhedral volumes diverge by less than 3% from the mean value. The octahedral distortion in these structures can be conveniently evaluated (Table 4) following Eby & Hawthorne (1993), who defined for copper oxysalts the parameter $\Delta = \frac{1}{6} \cdot \Sigma [\frac{(l_i - l_0)}{l_0}]^2$ where l_i represent the various Me-O bond distances, and l_o the mean bond distance in each polyhedron. It is evident from Table 4 that the polyhedral distortion is directly related, as expected, to the presence of copper, Me1 and Me2 polyhedra of malachite being the most distorted in each series.

Table 4. Site occupancy, polyhedral volume and distortion, derived from available structural data for the malachite-rosasite group.

	Me1 occupancy	vol.(Å^3)	Δ	Me2 occupancy	vol.(Å^3)	Δ	Ref
Glaukosphaerite	Cu 1	13.3	0.013762	$Ni_{0.5}Cu_{0.5}$	11.6	0.001614	(1)
Malachite	Cu 1	13.1	0.019209	Cu 1	11.8	0.005825	(2)
Mcguinnessite	$Cu_{0.85}Mg_{0.15}$	13.4	0.013403	$Mg_{0.85}Cu_{0.15}$	11.7	0.000773	(3)
Pokrovskite	$Mg_{0.88}$	13.1	0.001746	$Mg_{0.88}$	12.2	0.000528	(1)
Rosasite	Cu 1	12.9	0.011598	$Zn_{0.8}Cu_{0.2}$	12.5	0.001301	(3)
	mean value	13.2		mean value	11.9		

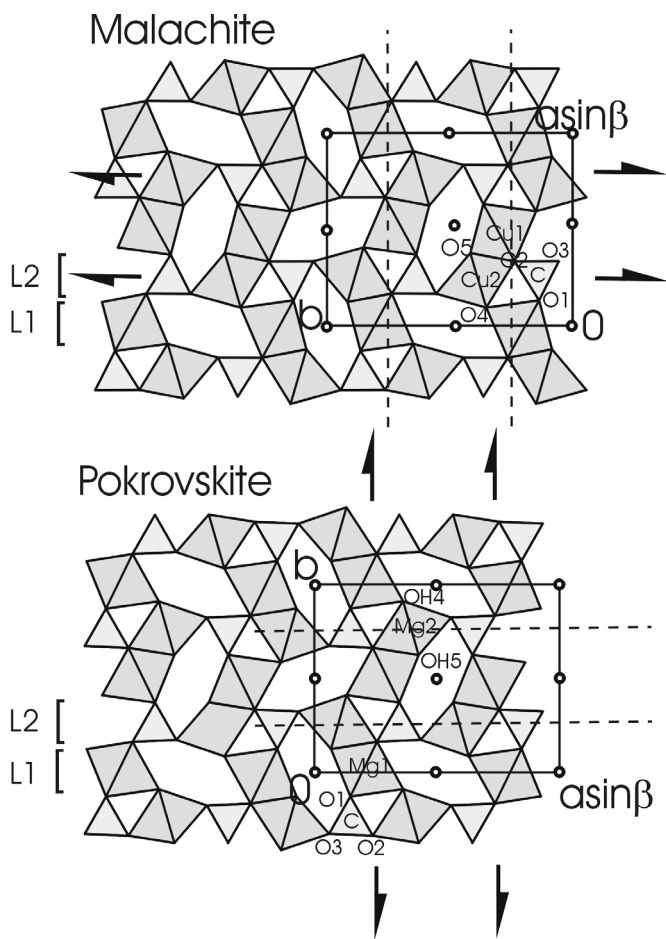(1) This study; (2) Zigan *et al.*, 1977; (3) Perchiazzi, 2006

Fig. 1. The crystal structures of malachite and pokrovskite, as seen along [001]. One can notice the different orientation of the space group operators in the structural framework of the two phases. L1 and L2 layers, regularly stacking along the ≈ 9.4 Å axis in both the two structures, are highlighted.

Fig. 2. Comparison of the L2 layers in pokroskite (a) and in malachite (b), as seen along their ≈ 9.4 Å axis. Both in malachite and pokrovskite the layers are made up by Me2 polyhedra and carbonate groups. It can be seen how octahedral columns and carbonate group inside each L2 layer are related by *a* glides in rosasite, and by 2_1 screw axes in malachite.

As stated above, two structure-types are realized in this mineral group, namely a malachite-like and a rosasite-like structure, the latter being realized in glaukosphaerite and pokrovskite. Given the isostructurality between glaukosphaerite and pokrovskite, in the following description of the polyhedral connections we shall refer to pokrovskite only, assuming its description is representative of glaukosphaerite too. The crystal structure of pokrovskite and malachite, as seen along [001], are compared in Fig. 1. As already noticed
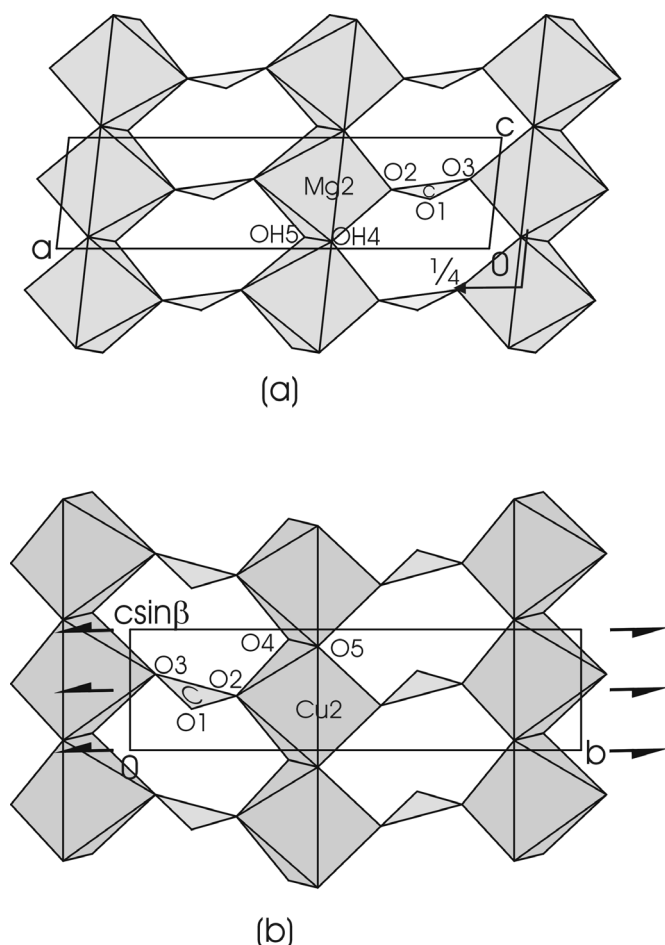
by Perchiazzi (2006), there is a close resemblance between these two structural types when seen in this projection. In both structures, Me1 and Me2 octahedra form, by edge-sharing, octahedral "ribbons", two columns wide and running along [001]. The "ribbons" are linked through corner-sharing to form corrugated "layers", parallel to (100) in pokrovskite and to (010) in malachite. Carbonate triangles are inserted between these corrugated layers, assuring an interlayer linkage.

Table 5. Bond valence balance (*v.u.*), calculated on the basis of the site occupancy for glaukosphaerite and pokrovskite. O···O distances (Å) and hydrogen bond strengths (*v.u.*) are reported.

	OH4···O3	*v.u.*		OH5···O1	*v.u.*
Pokrovskite	2.718 Å	0.22		2.792 Å	0.19
Glaukosphaerite	2.789 Å	0.19		2.629 Å	0.27

	O1	O2	O3	OH4	OH5
Pokrovskite	2.05	1.97	1.90	0.70	0.68
Glaukosphaerite	2.08	2.04	1.90	1.08	0.77

An alternative way of describing the polyhedral connections, following Perchiazzi (2006), refers to the L1 and L2 layers highlighted in Fig. 1: L1 layer is made up by the more distorted Me1 polyhedra, whereas L2 contains Me2 polyhedra and carbonate triangles. L1 and L2 layers, both with thickness $\approx b/4$ (with reference to the unit cell of pokrovskite) are regularly stacked along the $\approx$ 9.4 Å axis in both structure-types. One can notice the different orientation of the space group symmetry operators with respect to these layers. The differences between the malachite-like and pokrovskite-like structures (the same holds for glaukosphaerite, mcguinnessite and rosasite) can be better appreciated (Fig. 2) comparing their L2 layers as seen along the $\approx$ 9.4 Å axis. Adjacent M2 octahedral columns are related by a glides normal to **b** in pokrovskite and by 2_1 axes parallel to **b** in malachite; consequently the O2-O3 edges of the connecting carbonate groups are constantly pointing in one direction in pokrovskite, whereas they assume "zig-zag" orientations in malachite.

Hydrogen bonds play an essential rôle in stabilizing pokrovskite and glaukosphaerite structures. They were recognized by looking at those O···O distances shorter than 3.1 Å, and not belonging to the same coordination polyhedron. Hydrogen bond contributions to the valence balance were evaluated according to Ferraris & Ivaldi (1988) and are reported in Table 5 together with the total valence balance of the anions, calculated according to Breese & O'Keeffe (1991). It can be seen from Table 5 that hydroxyl groups are clearly distinguished from oxygens, and that the deviations of the valence sums from the ideal values are reasonable for all the anions in both compounds.

Discussion

The structural results here presented consent to confidently discuss a set of unsolved problems within the malachite-rosasite group of minerals.

Composition of pokroskvite

Ivanov *et al.* (1984) point to the formula $Mg_2(CO_3)(OH)_2 \cdot \frac{1}{2}H_2O$ for pokrovskite, on the basis of the chemical data and spectroscopic evidences. However the structural determination indicates that no site exists to host excess water molecules. The only possible way to locate more water than that corresponding to the ideal formula $Mg_2(CO_3)(OH)_2$ is by partial substitution of the hydroxyl anions by H_2O molecules, balancing the substitution with corresponding vacancies in the octahedral sites.

The study by Fitzpatrick (1986) of pokrovskite specimens from various North American localities confirms the relatively high water content which persists after prolonged heating at 110°C. In particular, the atomic contents presented by Fitzpatrick (1986) for the specimen from Sonoma, which is the object of the present paper, are: Me^{2+} 1.77 (more precisely Mg 1.62, Fe 0.09, Mn 0.06), C 0.97, H 2.56. Consequently the 'empirical' formula for pokrovskite from Sonoma is: $Me_{1.77}(CO_3)[(OH)_{1.54}/(H_2O)_{0.46}]$. Interestingly, the data of Fitzpatrick (1986) fully confirm the correlation between OH$^-$ by H_2O substitution and fraction of vacant octahedral sites.

Difficulties and ambiguities in powder pattern indexing

It is now evident that the problems met with in previous studies for reliably indexing powder patterns of glaukosphaerite and pokrovskite are largely due to the assumed isostructurality of the two phases with malachite. Actually, as it was described in the previous section of this paper and illustrated in Fig. 2, glaukosphaerite and pokrovskite display the structure-type of rosasite, neatly distinct from that of malachite as regards the position of the twofold axis, which is placed parallel to the ~12Å axis in malachite and parallel to the ~9.4Å axis in rosasite. The attempts to interpret the X-ray powder patterns of phases with rosasite structure-type on the basis of malachite-type cell parameters could be at least partially successful only through 'artificial' changes in the cell parameters (for example, an anomalously high value of c parameter) or by passing to a triclinic cell or by doubling the ~12Å parameter in a pseudo-orthorhombic cell.

In this context it is proper to recall that there are four distinct types of cells which may be referred to in the crystallographic description of phases with rosasite structure-type and whose knowledge is necessary to avoid mistakes or misunderstandings. The different cell parameters for the various possible settings are reported in Table 6 for glaukosphaerite. Cell type I corresponds to the setting used in the first successful indexing of rosasite powder pattern (Roberts *et al.*, 1986) and used for the structure determination and refinement of rosasite and mcguinessite by Perchiazzi (2006). Cell type III corresponds to the setting used in the present paper, which seems preferable due to the shorter a parameter and smaller β angle. It is interesting and useful to observe that another cell with quite similar parameters (cell type II) exists; however the space group symmetry of the structure in that setting is $P2_1/n$. Last, cell type IV is pseudo-orthorhombic and B centred and corresponds to the A centred orthorhombic cell found by Nickel & Berry (1981), once the **a** and **b** axis are exchanged.

Structure-type of other members of the malachite-rosasite group

The actual structural arrangements of few other phases [kolwezite $(Cu,Co)_2(CO_3)(OH)_2$, nullaginite $Ni_2(CO_3)(OH)_2$,

Table 6. Crystallographic parameters (Å and °) of glaucosphaerite in the various unit cells. For each cell-type the transformation matrix to obtain the corresponding parameters from those of the cell-type I is given.

Cell-type	a	b	c	β	Transformation matrix	
I	12.7881	9.3653	3.1361	110.966	[100/010/001]	$P2_1/a$
II	12.0279	9.3653	3.1361	96.875	[101/010/001]	$P2_1/n$
III	12.0613	9.3653	3.1361	98.085	[102/0$\bar{1}$0/00$\bar{1}$]	$P2_1/a$
IV	23.8842	9.3653	3.1361	89.384	[203/010/001]	B centred

and $Fe_2(CO_3)(OH)_2$] in the malachite-rosasite group still remain unknown, although reliable guesses may be drawn on the basis of the updated structural knowledge. A reliable assignement of phases to the malachite or rosasite structure-type may be easily done looking at a pair of highly distinctive lines in the powder patterns of the compounds with known structure: malachite, rosasite, mcguinessite, glaukosphaerite, pokrovskite. A strong reflection in malachite (PDF-41–1390) is $\bar{2}$ 01 at $d = 2.861$ Å, with $I = 73$, whereas no reflection or only very weak reflections are present in the d range 2.55 – 2.75 Å. On the contrary for the phases with rosasite structure-type a strong reflection is $\bar{1}$ 21 [with reference to the cell-type III] at $d = 2.58 – 2.61$ Å, with a largely weaker reflection 410 at $d = 2.84 – 2.87$ Å.

On these bases it may be confidently assumed that two phases with unknown structure-type, namely nullaginite (PDF 35–501, $d = 2.579$ Å, $I = 100$; $d = 2.854$ Å, $I = 20$), and kolwezite (PDF 29–1416, $d = 2.599$ Å, $I = 70$; $d = 2.84$–2.87 Å, absent), actually display the structure-type of rosasite.

References

Altomare, A., Calandro, R., Camalli, M., Cuocci, C., Giacovazzo, C., Gagliardi, A., Moliterni, A.G.G., Rizzi, R. (2004): Automatic structure determination from powder data with EXPO2004. *J. Appl. Cryst.* **37**,1025–1028.

Brese, N.E. & O'Keeffe, M. (1991) Bond-valence parameters for solids. *Acta Cryst.* **B47**, 192–197.

Burke, E.A.J. & Ferraris, G. (2005): New minerals approved in 2005 nomenclature modifications approved in 2005 by the Commission on new minerals and mineral names International Mineralogical Association. http://www.geo.vu.nl/~ima-cnmmn/minerals2005.pdf

Cheary, R.W. & Coelho, A.A.,(1992): A fundamental parameters approach to x-ray line-profile fitting *J. Appl. Cryst.* **25**, 109–121.

____, ____ (1998): Axial divergence in a conventional powder diffractometer. II. Realization and evaluation in a fundamental parameter profile fitting procedure. *J. Appl. Cryst.* **31**, 862–868.

Coelho, A.A. (2004): TOPAS-ACADEMIC, http://pws.prserv.net/Alan.Coelho/.

Deliens, M. & Piret, P. (1980) : La kolwesite, un hydrocarbonate de cuivre et de cobalt analogue a la glaukosphaerite et a la rosasite. *Bull. Min.* **103**, 179–184.

Dollase, W.A. (1986): Correction of intensities for preferred orientation in powder diffractometry: application of the March model. *J. Appl. Cryst.* **19**, 267–272.

Eby, R.K.& Hawthorne, F.C. (1993): Structural relations in copper oxysalt minerals. I. Structural hierarchy. *Acta Cryst.* **B49**, 28–56.

Erdös, V.E. & Altorfer, H. (1976): Ein dem Malachit ähnliches basisches Eisen-karbonat als Korrosionproduct von Stahl. *Werkstöffe und Korrosion* **27**, 304–312.

Ferraris, G. & Ivaldi, G. (1988): Bond valence *vs* bond length in O···O hydrogen bonds. *Acta Cryst.*, **B44**, 341–344.

Fitzpatrick, J.J. (1986) : Pokrovskite : its possible relatinship to mcguinnessite and the problem of excess water. 14th Meeting International Mineralogical Association, Abstracts, p. 101.

Gunter, J.R. & Oswald, H.R. (1977): Crystal structure of $Mg_2(OH)_2(CO_3)$, deduced from the topotactic thermal decomposition of artinite. *J. Solid State Chem.* **21**, 211–215

Ivanov, O.K., Malinovskii, Yu.A., Mozherin, Yu.V. (1984): Pokrovskite, $Mg_2(OH)_2(CO_3) \cdot ½ H_2O$, a new mineral from the Zlatagorskaya layered intrusive, Kazakhstan. *Zap. Vses. Min. Obsh.*, **113**, 90–95.

Jambor, J.L. (1976) : A possible unit cell for glaucosphaerite. *Can. Min.*, **14**, 574–576.

Nickel, E.H. & Berry, L.G. (1981) : The new mineral nullaginite and additional data on the related minerals rosasite and glaukosphaerite. *Can. Min.* **19**, 315–324.

Pawley, G.S. (1981): Unit-cell refinement from powder diffraction scans. *J. Appl. Cryst.* **14**, 357–361.

Perchiazzi, N. (2006): Crystal structure determination and Rietveld refinement of rosasite and mcguinnessite. *Zeit. Krist.* Supplement Issue n. 23, 505–510.

Pryce, M.W. & Just, J. (1974): Glaukosphaerite, a new nickel analogue of rosasite. *Min. Mag.* **39**, 737–743.

Roberts, A.C., Jambor, J.L., Grice, J.D. (1986): The X-ray crystallography of rosasite from Tsumeb, Namibia. *Pow. Diff.* **1**, 56–57.

Sabine, T.M., Hunter, B.A., Sabine , W.R., Ball, C.J. (1998): Analytical Expressions for the Transmission Factor and Peak Shift in Absorbing Cylindrical Specimens *J. Appl. Cryst.* **31**, 47 – 51.

White, J.S.(1987): Pokrovskite, a common mineral. *Min. Rec.* **18**, 135–136.

Zemann, J. (1981): Zür Stereochemie der Karbonate. *Fortschr. Mineral.* **59**, 95–116.

Zigan, F., Joswig, W., Schuster, H.D., Mason, S.A. (1977): Verfeinerung der Struktur von Malachit, $Cu_2(OH)_2CO_3$, durch neutronenbeugung. *Zeit. Krist.* **145**, 412–426.